

NLO QCD Corrections to B_c -to-Charmonium Form Factors

Cong-Feng Qiao¹ and Peng Sun^{1,2}, and Feng Yuan³

¹*College of Physical Sciences, Graduate University of Chinese Academy of Sciences
YuQuan Road 19A, Beijing 100049, China*

²*Center for High-Energy Physics, Peking University, Beijing 100871, China and*

³*Nuclear Science Division, LBNL, Berkeley, CA 94720, USA*

Abstract

The $B_c(^1S_0)$ meson to S-wave Charmonia transition form factors in large recoil region are calculated in next-to-leading order(NLO) accuracy of Quantum Chromodynamics(QCD). Our results indicate that the higher order corrections to these form factors are remarkable, and hence are important to the phenomenological study of the corresponding processes. For the convenience of comparison and use, the relevant expressions in asymptotic form in the limit of $m_c \rightarrow 0$ are presented.

PACS number(s): 12.38.Bx, 12.38.St, 12.39.Hg, 14.40.Nd.

I. INTRODUCTION

The study of B_c meson is of special interest, since it is the only heavy meson composed of two heavy quarks with different flavors. The B_c exclusive decays provide an important non-relativistic system in the investigation of weak interaction, hadronic properties of heavy mesons and even new physics. Up to now there are only two decay modes of B_c meson being observed in experiment at the Fermilab Tevatron, i.e. $B_c(1S_0) \rightarrow J/\psi\pi$ and $B_c(1S_0) \rightarrow J/\psi e^+\nu_e$ [1]. Theoretically, many of works were carried out in different frameworks, see for instance recent works [2, 3] and references therein. In analyzing the B_c decay processes, there are several different scales should be taken into account: the hard scale set by the heavy quark masses m_Q , the soft scale set by $m_Q v$ where $v < 1$ is the relative velocity of heavy quarks within the B_c meson, and the ultrasoft scale set by $m_Q v^2$. The hard part supplies the short-distance contribution and can be calculated perturbatively in strong interaction, while the soft and ultrasoft parts belong to the long-distance contribution and have to be evaluated via some non-perturbative methods or fitted by experimental data.

In the study of B -meson decays, the factorization [4, 5] is crucial to disentangle the short-distance sector from the long-distance sector, where the former can be treated by perturbative QCD(pQCD), while the later can be characterized by some universal hadronic parameters. Because B to light hadron exclusive decays are mediated by weak interaction, it is convenient to use an effective weak Hamiltonian to describe the interaction, which has the following structure:

$$\mathcal{H}_{eff} = \frac{G_F}{\sqrt{2}} \sum_i V_{CKM}^i C_i(\mu) Q_i. \quad (1)$$

Here G_F is the Fermi constant and Q_i are local operators, C_i are short-distance coefficients [6, 7] and V_{CKM}^i is CKM matrix element [8, 9]. In naive factorization approach, the B -meson exclusive two-body decays can be formulated as

$$\langle M_1 M_2 | Q_i | B \rangle \sim \langle M_1 | \bar{\psi} \Gamma b | B \rangle \langle M_2 | \bar{\psi} \Gamma \psi | 0 \rangle, \quad (2)$$

where the matrix element $\langle M_1 | \bar{\psi} \Gamma b | B \rangle$ stands for the transition form factor at large recoil, and $\langle M_2 | \bar{\psi} \Gamma \psi | 0 \rangle$ corresponds to the M_2 decay constant. If we consider all the partons on light-cone, the matrix element $\langle M_1 | \bar{\psi} \Gamma b | B \rangle$ can not be factorized further due to the divergence at the end point arising from vanishing energy of the partons on the light-cone.

However, if we extend to the non-relativistic situation, the nonperturbative effect can be factorized to Coulomb potentials of initial or final bound states. For instance, in the process $B_c \rightarrow J/\psi(\eta_c) + \pi$, we can describe the dynamics of bound states B_c and $J/\psi(\eta_c)$ by non-relativistic QCD(NRQCD) [10], since the masses of bottom and charm quarks are much bigger than Λ_{QCD} . And then, the matrix element relevant to the form factor at large recoil can be factorized as [11, 12]:

$$\langle J/\psi(\eta_c) | \bar{c} \Gamma_i b | B_c \rangle \simeq \psi_{B_c}(0) \psi_{J/\psi(\eta_c)}(0) T_i . \quad (3)$$

Here, the nonperturbative parameters $\psi_{\bar{B}_c}(0)$ and $\psi_{J/\psi(\eta_c)}(0)$ are the Schrödinger wave functions at the origin for $b\bar{c}$ and $c\bar{c}$ systems, respectively. T_i is a hard scattering kernel which can be calculated perturbatively.

As the LHC will soon be in the position to explore many B_c decay channels - among these several are in semileptonic and nonleptonic charmonium decay modes - a dedicated study of B_c -to-charmonium form factors is meaningful. In this work, we will explicitly calculate the matrix elements $\langle J/\psi | \bar{c} \Gamma_{V(A)} b | B_c \rangle$ and $\langle \eta_c | \bar{c} \Gamma_V b | B_c \rangle$ in pQCD approach at the next-to-leading order in non-relativistic limit of the initial and final bound states. The paper is organized as follows: in section II, we represent matrix element at the Born level; in section III, we calculate the matrix elements in the NLO accuracy in pQCD; in section IV, we compare result from pQCD with the wave-function overlap contribution qualitatively; in the last section a brief summary and conclusions are given.

II. THE FORM FACTORS AT BORN LEVEL

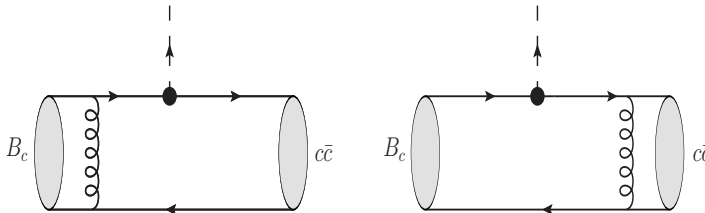


FIG. 1: The leading order Feynman diagrams

The investigation of process B_c decays to S-wave charmonia (J/ψ or η_c) with a light meson or lepton pair plays an important role in the study of B_c property, where the nature

of the transition form factor stands as a central issue. In this work, we focus on the study of two and four independent form factors in $B_c(1S_0)$ to η_c and J/ψ transitions respectively, which are normally defined as:

$$\langle \eta_c(P') | \bar{c} \gamma^\mu b | B_c(P) \rangle = f_+(P' + P)^\mu + f_-(P - P')^\mu, \quad (4)$$

$$\langle J/\psi(P', \epsilon^*) | \bar{c} \gamma^\mu b | B_c(P) \rangle = ig \epsilon^{\mu\nu\sigma\rho} \epsilon_\nu^* P_\sigma P'_\rho, \quad (5)$$

$$\langle J/\psi(P', \epsilon^*) | \bar{c} \gamma^\mu \gamma^5 b | B_c(P) \rangle = a_0 \epsilon^{*\mu} + a_+ \epsilon^* \cdot P P'^\mu + a_- \epsilon^* \cdot P P^\mu. \quad (6)$$

At the leading order in α_s , there are two independent Feynman Diagrams for $\langle J/\psi | \bar{c} \Gamma_{V(A)} b | B_c \rangle$ and $\langle \eta_c | \bar{c} \Gamma_{V(A)} b | B_c \rangle$, as schemetically shown in Figure 1. In non-relativistic limit, the momenta of constituent bottom and charm quarks are $p_b = \xi P$ and $p_{\bar{c}} = (1 - \xi)P$ with $\xi = \frac{m_b}{m_c + m_b}$ for B_c meson, and $p_{\bar{c}} = p_c = P'/2$ for J/ψ or η_c meson. Here, P and P' signify the momenta of initial B_c and final charmonia.

After taking the above mentioned procedures, it is straightforward to calculate those concerned form factors at the tree level. They read

$$f_+^{LO} = \frac{8\sqrt{2}\pi\alpha_s\psi(0)_{B_c}\psi(0)_{\eta_c}C_A C_F(\sqrt{m_b+m_c})(3m_b^2+2m_c m_b+3m_c^2-q^2)}{N_c m_c^{3/2}(m_b^2+m_c^2-2m_b m_c-q^2)^2}, \quad (7)$$

$$f_-^{LO} = -\frac{16\sqrt{2}\pi\alpha_s\psi(0)_{B_c}\psi(0)_{\eta_c}C_A C_F(m_b+m_c)^{3/2}(m_b-m_c)}{N_c m_c^{3/2}(m_b^2+m_c^2-2m_c m_b-q^2)^2}, \quad (8)$$

$$g^{LO} = -\frac{32\sqrt{2}\pi\alpha_s\psi(0)_{B_c}\psi(0)_{J/\psi}C_A C_F(m_b+m_c)^{3/2}}{N_c m_c^{3/2}(m_b^2+m_c^2-2m_c m_b-q^2)^2}, \quad (9)$$

$$a_0^{LO} = \frac{16\sqrt{2}\pi\alpha_s\psi(0)_{B_c}\psi(0)_{J/\psi}C_A C_F\sqrt{m_b+m_c}(m_b^3+6m_c m_b^2+5m_c^2 m_b-q^2 m_b+4m_c^3-2m_c q^2)}{N_c m_c^{3/2}(m_b^2+m_c^2-2m_c m_b-q^2)^2}, \quad (10)$$

$$a_+^{LO} = -\frac{32\sqrt{2}\pi\alpha_s\psi(0)_{B_c}\psi(0)_{J/\psi}C_A C_F(m_b+m_c)^{3/2}}{N_c m_c^{3/2}(m_b^2+m_c^2-2m_c m_b-q^2)^2}, \quad (11)$$

$$a_-^{LO} = \frac{32\sqrt{2}\pi\alpha_s\psi(0)_{B_c}\psi(0)_{J/\psi}C_A C_F\sqrt{m_b+m_c}}{N_c\sqrt{m_c}(m_b^2+m_c^2-2m_c m_b-q^2)^2}. \quad (12)$$

Here, the momentum transfer $q = P - P'$, and the invariant mass $q^2 \rightarrow 0$, i.e. the final charmonium owns the maximal momentum, denotes the maximum recoil point.

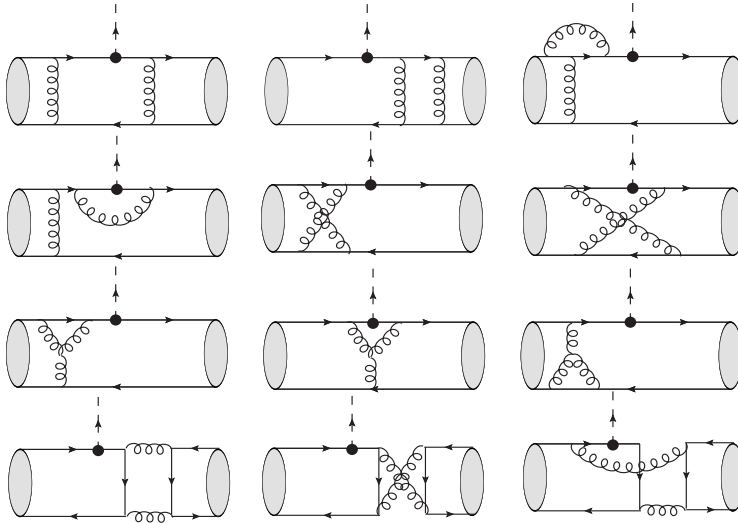


FIG. 2: The typical Feynman diagrams at one-loop level.

III. THE NEXT-TO-LEADING ORDER CORRECTIONS

In performing the next-to-leading order calculation, as schematically shown in Figure 2, we use the dimensional regularization scheme to regularize the UV and IR divergences, and the Coulomb divergence is regularized by the relative velocity v . In dimensional regularization, it is well-known that the γ_5 is difficult to deal with. In the literature, two approaches are mostly employed, that is the Naive scheme [13] and the 't Hooft-Veltman scheme [14]. In this calculation, we adopt the Naive scheme, of which the γ_5 anticommutes with each γ^μ matrix in d-dimension space-time, $\{\gamma_5, \gamma^\mu\} = 0$. In evaluating the quarkonium production and decays, it was argued by Ref. [15] that both schemes may lead to the same result, which is different from the case of pion decays to di-photon. The UV divergences exist merely in self-energy and triangle diagrams, which can be renormalized by the corresponding counter terms. The renormalization constants include Z_2 , Z_3 , Z_m , and Z_g , referring to quark field, gluon field, quark mass, and strong coupling constant α_s , respectively. In our calculation the Z_g is defined in the modified-minimal-subtraction ($\overline{\text{MS}}$) scheme, while for the other three

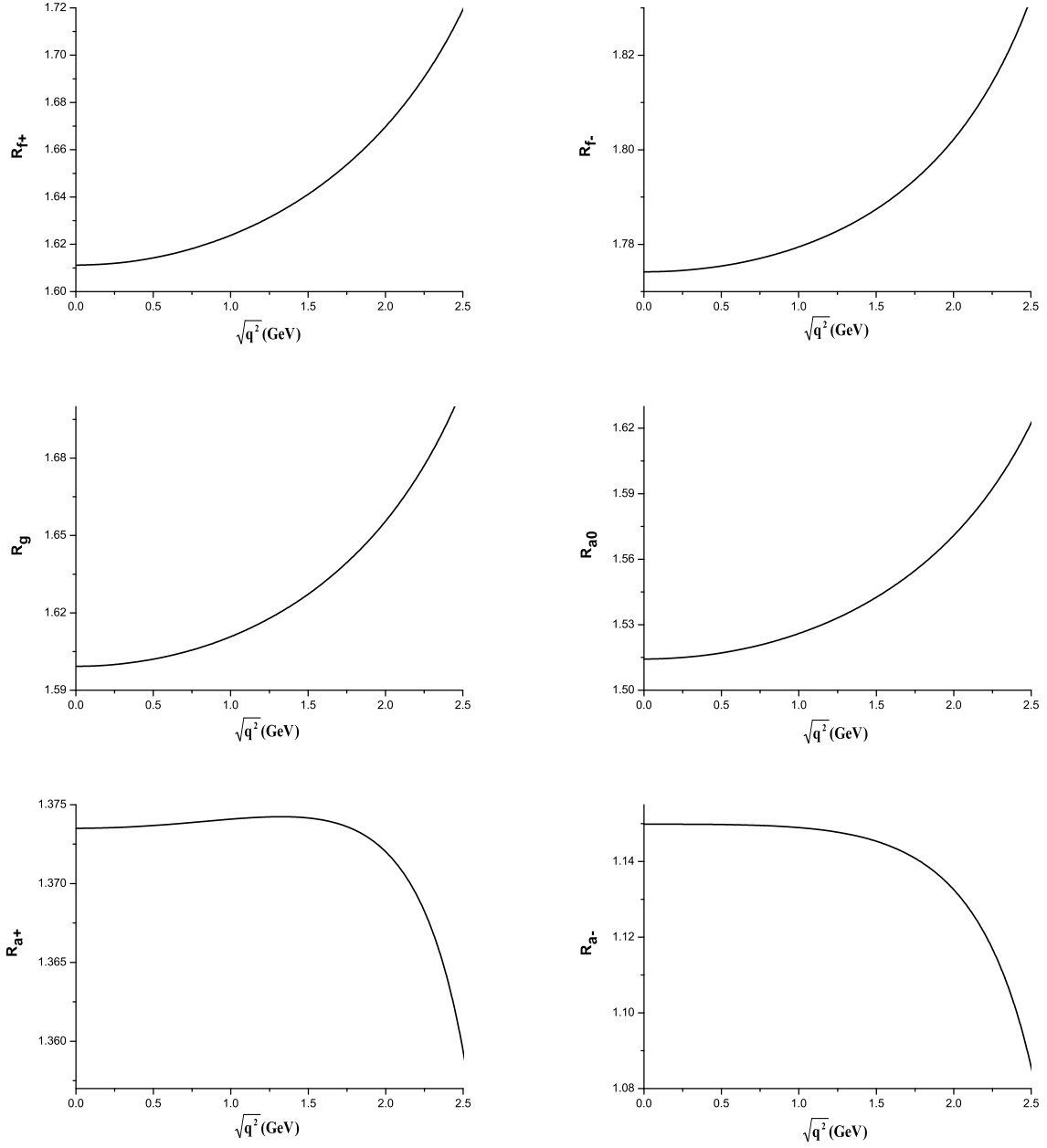


FIG. 3: The ratios of NLO and LO form factors vs the square root of momentum transfer $\sqrt{q^2}$. Here, $R_i(q^2) = \frac{F_i^{NLO}(q^2)}{F_i^{LO}(q^2)}$ with F_i standing for f_+ , f_- , g , a_0 , a_+ , and a_- . The renormalization-scale is fixed at $\mu = 3$ GeV; $m_b = 4.76$ GeV and $m_c = 1.54$ GeV is adopted.

the on-shell (OS) scheme is employed, which tells

$$\begin{aligned}
\delta Z_m^{OS} &= -3C_F \frac{\alpha_s}{4\pi} \left[\frac{1}{\epsilon_{UV}} - \gamma_E + \ln \frac{4\pi\mu^2}{m^2} + \frac{4}{3} + \mathcal{O}(\epsilon) \right] , \\
\delta Z_2^{OS} &= -C_F \frac{\alpha_s}{4\pi} \left[\frac{1}{\epsilon_{UV}} + \frac{2}{\epsilon_{IR}} - 3\gamma_E + 3 \ln \frac{4\pi\mu^2}{m^2} + 4 + \mathcal{O}(\epsilon) \right] , \\
\delta Z_3^{OS} &= \frac{\alpha_s}{4\pi} \left[(\beta_0 - 2C_A) \left(\frac{1}{\epsilon_{UV}} - \frac{1}{\epsilon_{IR}} \right) + \mathcal{O}(\epsilon) \right] , \\
\delta Z_g^{\overline{MS}} &= -\frac{\beta_0}{2} \frac{\alpha_s}{4\pi} \left[\frac{1}{\epsilon_{UV}} - \gamma_E + \ln 4\pi + \mathcal{O}(\epsilon) \right] .
\end{aligned} \tag{13}$$

Here, $\beta_0 = (11/3)C_A - (4/3)T_f n_f$ is the one-loop coefficient of the QCD beta function; $n_f = 3$ is the number of active quarks in our calculation; $C_A = 3$ and $T_F = 1/2$ attribute to the SU(3) group; μ is the renormalization scale.

Because in our calculation the m_c/m_b contribution is kept, the complete expression turns to be too lengthy to be presented here. Whereas, the asymptotic form in small m_c limit is given in the appendix, and the numerical results are presented. From the asymptotic form a noteworthy finding is that there exists an interesting relation among those form factors, i.e,

$$\frac{a_0^{NLO}}{a_0^{LO}} = \frac{a_+^{NLO}}{a_+^{LO}} = \frac{g^{NLO}}{g^{LO}} , \tag{14}$$

which is consistent with the prediction of Ref.[16] from large energy effective theory(LEET).

In numerical calculation, the input heavy quark masses are

$$m_b = 4.76 \text{ GeV}, \quad m_c = 1.54 \text{ GeV} . \tag{15}$$

The one loop result for strong coupling constant, the

$$\alpha_s(\mu) = \frac{4\pi}{(11 - \frac{2}{3}n_f) \text{Log}(\frac{\mu^2}{\Lambda_{QCD}^2})} . \tag{16}$$

is used.

In Figure 3, the ratios of NLO and LO form factors versus the square root of momentum transfer $\sqrt{q^2}$ are schematically shown, while it should be noted that the pQCD approach is feasible only in the maximum recoil region. The figure shows that the NLO corrections to the B_c to charmonia transition form factors are remarkable and sensitive to the momentum transfer q . The renormalization-scale dependence of the LO and NLO form factors are

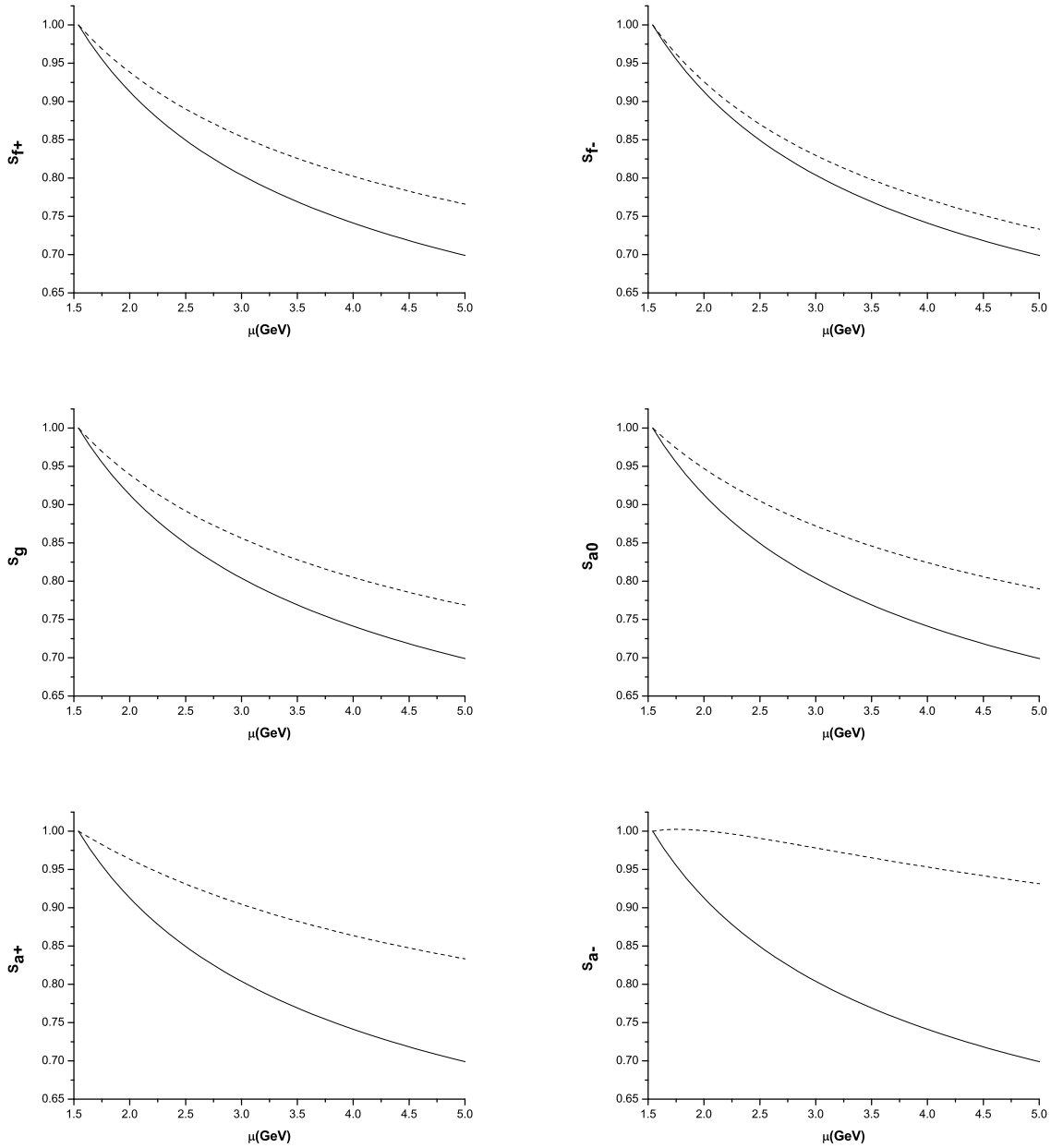


FIG. 4: The renormalization-scale dependence of the LO and NLO form factors at the maximum recoil point, $q^2 = 0$. Here, $S_i(\mu) = \frac{F_i(\mu)}{F_i(m_c)}$ with F_i standing for f_+ , f_- , g , a_0 , a_+ , and a_- . The solid line represents the situation of the LO renormalization-scale dependence and the dash line represents for the NLO situation. In the computation, $m_b = 4.76$ GeV and $m_c = 1.54$ GeV are adopted.

presented in Figure 4 at the maximum recoil point $q^2 = 0$. Generally speaking, the scale dependence in NLO is obviously depressed relative to the LO case.

To show more explicitly the difference of LO and NLO results, we employ the function of $S_{\text{R}}^i(\mu) = 4\pi\alpha_s(\mu)\frac{F_i(\mu)}{F_i^{\text{LO}}(\mu)}$ to exhibit the dependence of renormalization-scale at the maximum

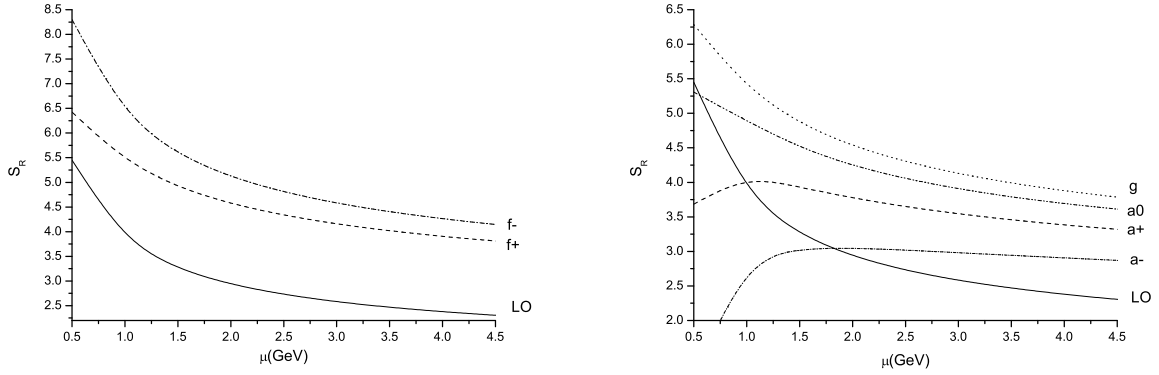


FIG. 5: The renormalization-scale dependence of the LO and NLO form factors at the maximum recoil point, $q^2 = 0$. Here, $S_R^i(\mu) = 4\pi\alpha_s \frac{F_i(\mu)}{F_i^{LO}(\mu)}$ with F_i standing for f_+ , f_- , g , a_0 , a_+ , and a_- . The symbol “LO” denotes the LO renormalization-scale running of $S_R^i(\mu)$. In the computation, $m_b = 4.76$ GeV and $m_c = 1.54$ GeV are adopted.

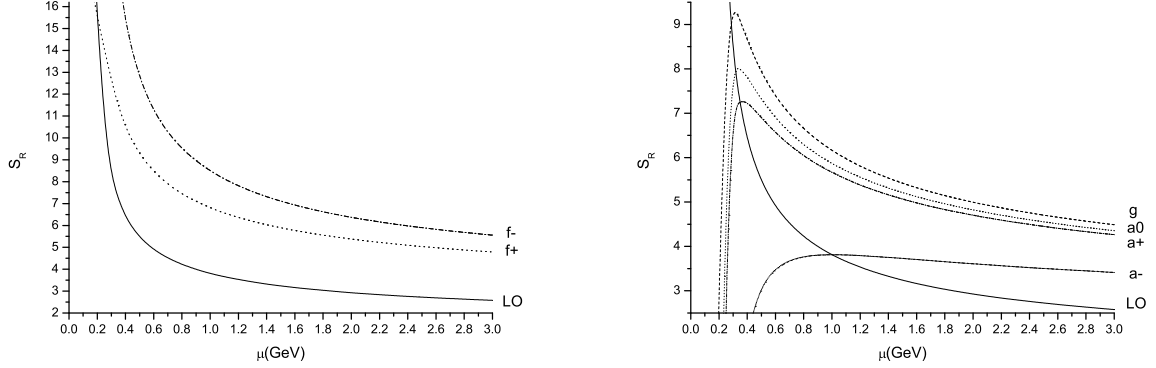


FIG. 6: The renormalization-scale dependence of the LO and NLO form factors at the maximum recoil point, $q^2 = 0$. In the computation, $m_b = 5$ GeV and $m_c = 0.3$ GeV are adopted and $S_R^i(\mu)$ is performed to all orders of m_c/m_b .

recoil $q^2 = 0$, as shown in Figures 5 to 7, where $F_i(\mu)$ stands for $F_i^{LO}(\mu)$ or $F_i^{LO}(\mu) + F_i^{NLO}(\mu)$ corresponding to LO renormalization-scale dependence and NLO one respectively. To test the validity of m_c/m_b expansion, giving m_c a nonphysical small mass we present in Figures 6 and 7 the leading order and full order results, respectively. From these figures we see that those form factors are quite sensitive to the magnitude of m_c , and the higher order effects in m_c/m_b expansion are notable.

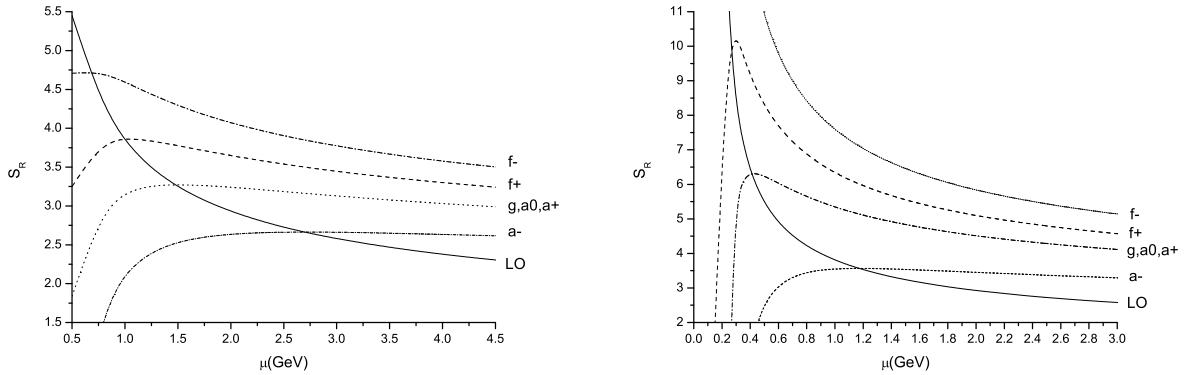


FIG. 7: The renormalization-scale dependence of the LO and NLO form factors at the maximum recoil point, $q^2 = 0$. The left one is for $m_b = 4.76$ GeV and $m_c = 1.54$ GeV; the right one for $m_b = 5$ GeV and $m_c = 0.3$ GeV; and the $S_R^i(\mu)$ is performed to the leading order of m_c/m_b .

In our calculation the package FeynArts [17] was used to generate the Feynman diagrams, the FeynCalc [18] was used to generate the amplitudes, and the LoopTools [19] was employed to calculate the Passarino-Veltman integrals.

IV. WAVE FUNCTION OVERLAP CONTRIBUTION

The wave function overlap contribution for B_c decays has been broadly discussed in the literature [20–33]. Since in the overlap contribution the QCD non-perturbative effects tend to be important, from pQCD factorization point of view it is beyond the scope of our interest in this work. However, here we still make a schematic comparison of the wave-function overlap contribution with pQCD contribution to the form factors for readers convenience.

From the Table I, we notice that the results from wave function overlap are comparable to what from the pQCD calculation at the maximum recoil point, though in fact they attribute to different mechanisms in the study of B_c decays.

TABLE I: $B_c \rightarrow \eta_c$ and J/ψ form factors at maximum recoil $q^2 = 0$ from pQCD and wave function overlap [33].

	$ F^{B_c \eta_c} $	$ A_0^{B_c J/\psi} $	$ A_1^{B_c J/\psi} $	$ A_2^{B_c J/\psi} $	$ V^{B_c J/\psi} $
DW[20] ^a	0.420	0.408	0.416	0.431	0.591
CNP[21]	0.20	0.26	0.27	0.28	0.38
KT[22]	0.23	0.21	0.21	0.23	0.33
KLO[23] ^b	0.66	0.60	0.63	0.69	1.03
NW[24]	0.5359	0.532	0.524	0.509	0.736
IKS[25]	0.76	0.69	0.68	0.66	0.96
Kiselev[26] ^c	0.66[0.7]	0.60[0.66]	0.63[0.66]	0.69[0.66]	1.03[0.94]
EFG[27]	0.47	0.40	0.50	0.73	0.49
IKS2[28]	0.61	0.57	0.56	0.54	0.83
HNV[29]	0.49	0.45	0.49	0.56	0.61
HZ[30]	0.87	0.27	0.75	1.69	1.69
SDY[31]	0.87	0.27	0.75	1.69	1.69
DSV[32]	0.58	0.58	0.63	0.74	0.91
WSL[33]	0.61	0.53	0.50	0.44	0.74
pQCD(LO) ^d	0.97	0.86	0.90	0.97	0.32
pQCD(NLO) ^d	1.57	1.34	1.35	1.39	0.52

^aWe quote the results with $\omega = 0.6$ GeV.

^bWe quote the values where the Coulomb corrections are taken into account.

^cThe results out (in) the brackets are evaluated in sum rules (potential model).

^d $\psi_{B_c}(0) = 0.36$ GeV^{3/2}, $\psi_{J/\psi}(0) = 0.26$ GeV^{3/2}, $\alpha_s = 0.2$

V. SUMMARY AND CONCLUSIONS

In this work we have calculated the transition form factors of the B_c meson to S-wave charmonia in the degree of NLO accuracy of pQCD. In our calculation, the B_c meson and charmonia are treated as non-relativistic bound states of two heavy quarks. Hence, the long-distance effects for the form factors come only from the soft gluon exchange between heavy quarks, which can be explicitly factorized out and expressed as the wave functions at

the origin. The factorization scale is set to be at vm_c in practical calculation, although the scale dependence does not appear at the one-loop level. Since in the small recoil region the end-point divergence spoils the QCD factorization, our result is valid only in the large recoil case.

Calculation shows that the NLO QCD corrections to the B_c to charmonia form factors are remarkable, especially for the f_- where the correction is as large as 80% or so. We find that the renormalization-scale dependence of the form factors are depressed, as it should be, when the next-to-leading order correction is taken into account, which means the uncertainties in the theoretical estimation are reduced. We find that B_c to charmonia transition form factors are quite sensitive to the magnitude of m_c , and the higher order effects in m_c/m_b expansion are indispensable.

Last, it should be mentioned that the relativistic corrections are also important for the B_c to charmonia form factors, which are highly related to the relative velocity of heavy quarks within the bound states, i.e. $v_{bc}^2 \sim 0.38$ and $v_{cc}^2 \sim 0.25$ for B_c and charmonium, respectively.

Acknowledgments

We thank De-Shan Yang and Rui-Lin Zhu for useful discussion and independent check of our result. This work was supported in part by the National Natural Science Foundation of China(NSFC) under the grants 10935012, 10928510, 10821063 and 10775179, by the CAS Key Projects KJCX2-yw-N29 and H92A0200S2.

Appendix

Following, various B_c to charmonium transition form factors are given in leading power of m_c/m_b and NLO pQCD. For the sake of compactness, we define $s = \frac{m_b^2}{m_b^2 - q^2}$ and $\gamma = \frac{m_b^2 - q^2}{4m_b m_c}$. It is worth emphasizing that our expressions for $\frac{f_+^{NLO}}{f_+^{LO}}$ and $\frac{f_-^{NLO}}{f_-^{LO}}$ agree with what given in

reference [12].

$$\begin{aligned}
\frac{f_+^{NLO}(q^2)}{f_+^{LO}(q^2)} &= 1 + \frac{\alpha_s}{4\pi} \left\{ \frac{1}{3} (11C_A - 2n_f) \log\left(\frac{\mu^2}{2\gamma m_c^2}\right) - \frac{10n_f}{9} + \frac{(\pi^2 - 6\log(2))(s-1) + 3s\log(\gamma)}{6s+3} \right. \\
&+ \frac{C_A}{72s^2 - 18} (18s^2(2s-1)\log^2(s) + 18(8\log(2)s^3 - 2\log(2)s^2 - 5\log(2)s + s \\
&+ 2\log(2))\log(s) + (2s-1)(268s + \pi^2(6s^2 - 3s - 6) + 170) - 9(2s \\
&- 1)\log(\gamma)(\log(\gamma)s - (2 + 2\log(2))s + 4\log(2)) + 18(2s-1)(4s^2 + s \\
&- 2)\text{Li}_2(1-2s) - 18(4s^3 - 5s + 2)\text{Li}_2(1-s) + 18(s(4s(s+1) - 11) \\
&+ 4)\log^2(2) - 36(5(s-1)s + 1)\log(2)) \\
&+ \frac{C_F}{6(1-2s)^2(2s+1)} (-6(2(s-1)s-1)\log^2(s)(1-2s)^2 + 3\log(\gamma)(23s \\
&+ (5s-2)\log(\gamma) - 4(s+1)\log(2) + 12)(1-2s)^2 - 12(4s^2 + s \\
&- 2)\text{Li}_2(1-2s)(1-2s)^2 + 12(s(2s+3) - 1)\text{Li}_2(1-s)(1-2s)^2 \\
&- (\pi - 2\pi s)^2(s(4s-19) + 4) + 3(-32\log^2(2)s^4 - 4(69 + 2\log(2)(-37 \\
&+ 5\log(2)))s^3 + 8(18 + \log(2)(-31 + 9\log(2)))s^2 + (61 + 28\log(2) \\
&- 26\log^2(2))s + 12\log(2) + 2\log^2(2) - 32) + (6s(8s(s(-4\log(2)s \\
&+ 3\log(2) + 3) + 2\log(2) - 3) - 18\log(2) + 7) + 24\log(2))\log(s) \left. \right\} \quad (17)
\end{aligned}$$

$$\begin{aligned}
\frac{f_+^{NLO}(0)}{f_+^{LO}(0)} &= 1 + \frac{\alpha_s}{4\pi} \left\{ \frac{1}{3} (11C_A - 2n_f) \log\left(\frac{2\mu^2}{m_b m_c}\right) - \frac{10n_f}{9} + \frac{1}{3} \log\left(\frac{m_b}{m_c}\right) - \frac{2\log(2)}{3} \right. \\
&+ C_F \left(\frac{1}{2} \log^2\left(\frac{m_b}{m_c}\right) - \frac{10}{3} \log(2) \log\left(\frac{m_b}{m_c}\right) + \frac{35}{6} \log\left(\frac{m_b}{m_c}\right) + \frac{2\log^2(2)}{3} \right. \\
&+ 3\log(2) + \frac{7\pi^2}{9} - \frac{103}{6} \left. \right) \\
&+ C_A \left(-\frac{1}{6} \log^2\left(\frac{m_b}{m_c}\right) + \frac{1}{3} \log(2) \log\left(\frac{m_b}{m_c}\right) + \frac{1}{3} \log\left(\frac{m_b}{m_c}\right) + \frac{\log^2(2)}{3} \right. \\
&- \frac{4\log(2)}{3} - \frac{5\pi^2}{36} + \frac{73}{9} \left. \right) \quad (18)
\end{aligned}$$

$$\begin{aligned}
\frac{f_-^{NLO}(q^2)}{f_-^{LO}(q^2)} &= 1 + \frac{\alpha_s}{4\pi} \left\{ \frac{1}{3} (11C_A - 2n_f) \log\left(\frac{\mu^2}{2\gamma m_c^2}\right) - \frac{10n_f}{9} + \frac{1}{6} (3\log(\gamma) - 6\log(2) + \pi^2) \right. \\
&+ \frac{C_A}{36(s-1)(2s-1)} (18(s-1)s(2s-1)\log^2(s) + 18((2s(4s-5)+1)\log(2)s \\
&+ s + \log(2) + 1)\log(s) + (s-1)(2s-1)(\pi^2(6s-3) + 268) \\
&+ 9(s-1)(2s-1)(-\log(\gamma) + 2\log(2) + 2)\log(\gamma) + 18(8s^3 - 10s^2 + s \\
&+ 1)\text{Li}_2(1-2s) - 18(s-1)(2s-1)(2s+1)\text{Li}_2(1-s) + 18(4s^3 - 7s \\
&+ 3)\log^2(2) - 36(s-1)(5s-1)\log(2)) \\
&- \frac{C_F}{12(1-2s)^2(s-1)^2} (12(1-2s)^2\log^2(s)(s-1)^3 + (\pi^2(s-1)(4s-19)(1-2s)^2 \\
&+ 3(32\log^2(2)s^4 + 4(69 + 2(-37 + \log(2))\log(2))s^3 + (-508 - 8\log(2)(-74 \\
&+ 13\log(2)))s^2 + (307 - 364\log(2) + 82\log^2(2))s + 2(34 - 9\log(2))\log(2) \\
&- 61))(s-1) + 6(s(s(-24s^2 + 84s + 2(2s-1)(2s(4s-9) + 11)\log(2) - 127) \\
&- 4\log(2) + 73) + 2\log(2) - 13)\log(s) + 3(2s^2 - 3s + 1)^2(-5\log(\gamma) + 4\log(2) \\
&- 23)\log(\gamma) + 12(4s+1)(2s^2 - 3s + 1)^2\text{Li}_2(1-2s) \\
&- 12(2s+3)(2s^2 - 3s + 1)^2\text{Li}_2(1-s)) \tag{19}
\end{aligned}$$

$$\begin{aligned}
\frac{f_-^{NLO}(0)}{f_-^{LO}(0)} &= 1 + \frac{\alpha_s}{4\pi} \left\{ \frac{1}{3} (11C_A - 2n_f) \log\left(\frac{2\mu^2}{m_b m_c}\right) - \frac{10n_f}{9} + \frac{1}{2} \log\left(\frac{m_b}{m_c}\right) - 2\log(2) + \frac{\pi^2}{6} \right. \\
&+ C_F \left(\frac{5}{4} \log^2\left(\frac{m_b}{m_c}\right) - 6\log(2)\log\left(\frac{m_b}{m_c}\right) + \frac{23}{4} \log\left(\frac{m_b}{m_c}\right) + \frac{\log^2(2)}{2} \right. \\
&+ \left. \frac{11\log(2)}{2} + \frac{5\pi^2}{3} - 19 \right) \\
&+ C_A \left(-\frac{1}{4} \log^2\left(\frac{m_b}{m_c}\right) + \frac{3}{2} \log(2)\log\left(\frac{m_b}{m_c}\right) + \frac{1}{2} \log\left(\frac{m_b}{m_c}\right) + \frac{\log^2(2)}{2} \right. \\
&- \left. 5\log(2) - \frac{\pi^2}{8} + \frac{76}{9} \right) \tag{20}
\end{aligned}$$

$$\begin{aligned}
\frac{g^{NLO}(q^2)}{g^{LO}(q^2)} &= 1 + \frac{\alpha_s}{4\pi} \left\{ \frac{1}{3} (11C_A - 2n_f) \log\left(\frac{\mu^2}{2\gamma m_c^2}\right) - \frac{10n_f}{9} \right. \\
&\quad - \frac{C_A}{36s - 18} (9s(2s - 1) \log^2(s) + 18(2s \log(2)(2s - 1) + 1) \log(s) \\
&\quad + 3\pi^2(s + 2)(2s - 1) - 2s(-18 \log^2(2)s + 9 \log^2(2) + 45 \log(2) + 134) \\
&\quad + 9(2s - 1)(\log(\gamma) - 3) \log(\gamma) + 18s(2s - 1)(2\text{Li}_2(1 - 2s) - \text{Li}_2(1 - s)) \\
&\quad + 63 \log(2) + 134) \\
&\quad - \frac{C_F}{6(1 - 2s)^2(s - 1)} (6(s^2 - 1) \log^2(s)(1 - 2s)^2 + 24(s - 1)s \text{Li}_2(1 - 2s)(1 - 2s)^2 \\
&\quad + 3(2s(s(4s(4 \log(2)s - 8 \log(2) + 3) + 20 \log(2) - 17) - 4 \log(2) + 7) - 1) \log(s) \\
&\quad + (s - 1)(6 \log(\gamma)(\log(\gamma) - 6 \log(2) + 5)(1 - 2s)^2 + 6(2s - 9) \log^2(2)(1 - 2s)^2 \\
&\quad + (2s - 1)(-204s + 2\pi^2(2s^2 + s - 1) + 105) + 6(s(68s - 67) + 16) \log(2)) \\
&\quad \left. - 12(2s^2 - 3s + 1)^2 \text{Li}_2(1 - s) \right\} \tag{21}
\end{aligned}$$

$$\begin{aligned}
\frac{g^{NLO}(0)}{g^{LO}(0)} &= 1 + \frac{\alpha_s}{4\pi} \left\{ \frac{1}{3} (11C_A - 2n_f) \log\left(\frac{2\mu^2}{m_b m_c}\right) - \frac{10n_f}{9} \right. \\
&\quad + C_F \left(\log^2\left(\frac{m_b}{m_c}\right) - 10 \log(2) \log\left(\frac{m_b}{m_c}\right) + 5 \log\left(\frac{m_b}{m_c}\right) + 9 \log^2(2) \right. \\
&\quad \left. + 7 \log(2) + \frac{\pi^2}{3} - 15 \right) \\
&\quad + C_A \left(-\frac{1}{2} \log^2\left(\frac{m_b}{m_c}\right) + 2 \log(2) \log\left(\frac{m_b}{m_c}\right) + \frac{3}{2} \log\left(\frac{m_b}{m_c}\right) - 3 \log^2(2) \right. \\
&\quad \left. - \frac{3 \log(2)}{2} - \frac{\pi^2}{3} + \frac{67}{9} \right) \tag{22}
\end{aligned}$$

$$\frac{a_0^{NLO}(q^2)}{a_0^{LO}(q^2)} = \frac{a_+^{NLO}(q^2)}{a_+^{LO}(q^2)} = \frac{g^{NLO}(q^2)}{g^{LO}(q^2)} \tag{23}$$

$$\frac{a_0^{NLO}(0)}{a_0^{LO}(0)} = \frac{a_+^{NLO}(0)}{a_+^{LO}(0)} = \frac{g^{NLO}(0)}{g^{LO}(0)} \tag{24}$$

$$\begin{aligned}
\frac{a_-^{NLO}(q^2)}{a_-^{LO}(q^2)} &= 1 + \frac{\alpha_s}{4\pi} \left\{ \frac{1}{3} (11C_A - 2n_f) \log\left(\frac{\mu^2}{2\gamma m_c^2}\right) - \frac{10n_f}{9} \right. \\
&\quad - \frac{C_A}{9(s-1)(2s-1)} (18(2\log(2)s^2 - 3\log(2)s + s + \log(2)) \log(s) \\
&\quad + (s-1)(2(-85 + 36(-1 + \log(2)) \log(2))s + \pi^2(6s-3) + 18(2s-1) \log(2) \log(\gamma) \\
&\quad - 18\log(2)(-1 + 2\log(2)) + 85) + 18(s-1)(2s-1) \text{Li}_2(1-2s) \\
&\quad \left. - 18(s-1)(2s-1) \text{Li}_2(1-s) \right) \\
&\quad + \frac{C_F}{(2s^2 - 3s + 1)^2} (\log^2(s)(2s^2 - 3s + 1)^2 + 4\text{Li}_2(1-2s)(2s^2 - 3s + 1)^2 \\
&\quad - 2\text{Li}_2(1-s)(2s^2 - 3s + 1)^2 + (s(s(4(3 + 4\log(2))s^2 - 8(5 + 6\log(2))s \\
&\quad + 52\log(2) + 27) - 4(1 + 6\log(2))) + 4\log(2)) \log(s) + \frac{1}{3}(12(-13 \\
&\quad + 2\log(2) + \log^2(2))s^4 - 12(-43 + 5\log(2) + 3\log^2(2))s^3 + (-597 \\
&\quad + 54\log(2) + 26\log(2)^2)s^2 - 3(-95 + 6\log^2(2) + 8\log(2))s \\
&\quad - 2\pi^2(2s^2 - 3s + 1)^2 - 3(2s^2 - 3s + 1)^2 \log(\gamma)(\log(\gamma) + 2\log(2) - 6) \\
&\quad \left. + 3\log^2(2) + 6\log(2) - 48) \right) \tag{25}
\end{aligned}$$

$$\begin{aligned}
\frac{a_-^{NLO}(0)}{a_-^{LO}(0)} &= 1 + \frac{\alpha_s}{4\pi} \left\{ \frac{1}{3} (11C_A - 2n_f) \log\left(\frac{2\mu^2}{m_b m_c}\right) - \frac{10n_f}{9} \right. \\
&\quad + C_F \left(-\log^2\left(\frac{m_b}{m_c}\right) + 2\log(2) \log\left(\frac{m_b}{m_c}\right) + 6\log\left(\frac{m_b}{m_c}\right) + \log^2(2) \right. \\
&\quad \left. - 6\log(2) - \pi^2 - \frac{29}{2} \right) \\
&\quad \left. + C_A \left(-2\log(2) \log\left(\frac{m_b}{m_c}\right) + 6\log(2) - \frac{\pi^2}{6} + \frac{67}{9} \right) \right) \tag{26}
\end{aligned}$$

-
- [1] T. Aaltonen et al. (CDF Collaboration), Phys. Rev. Lett. **100**, 182002 (2008); A. Abulencia et al. (CDF Collaboration), Phys. Lett. **97**, 012002 (2006); V. M. Abazov et al. (D0 Collaboration), Phys. Rev. Lett. **102**, 092001 (2009).
- [2] I. Bediaga and J. H. Munoz, arXiv:1102.2190.
- [3] X. Liu, Z. J. Xiao, and C. D. Lu, Phys. Rev. D **81**, 014022 (2010).
- [4] A. J. Buras, arXiv:hep-ph9806471.
- [5] M. Beneke, G. Buchalla, M. Neubert and C. T. Sachrajda, Phys. Rev. Lett. **83**, 1914 (1999); Nucl. Phys. **B591**, 313 (2000); Nucl. Phys. **B606**, 245 (2001).
- [6] K. G. Wilson, Phys. Rev. **179**, 1499 (1969); K. G. Wilson and W. Zimmermann, Comm. Math. Phys. **24**, 87 (1972).
- [7] W. Zimmermann, in Proc. 1970 Brandeis Summer Institute in Theor. Phys, (eds. S. Deser, M. Grisaru and H. Pendleton), MIT Press, 1971, p.396; Ann. Phys. **77**, 570 (1973).
- [8] N. Cabibbo, Phys. Rev. Lett. **10**, 531 (1963).
- [9] M. Kobayashi and K. Maskawa, Pro. Theor. Phys. **49**, 652 (1973).
- [10] G.T. Bodwin, E. Braaten, and G. P. Lepage, Phys. Rev. D **51**, 1125 (1995).
- [11] G. Bell and Th. Feldmann, Nuclear Physics B (Proc. Suppl.) **164**, 189 (2007).
- [12] G. Bell, arXiv:0705.3133.
- [13] M. S. Chanowitz, M. Furman and I. Hinchliffe, Nucl. Phys. B **159**, 225 (1979).
- [14] G. 't Hooft and M. J. G. Veltman, Nucl. Phys. B **44**, 189 (1972).
- [15] A. Petrelli, M. Cacciari, M. Greco, F. Maltoni and M. L. Mangano, Nucl. Phys. B **514**, 245 (1998)
- [16] J. Charles, A. Le Yaouanc, L. Oliver, O. Pene and J. C. Raynal, Phys. Rev. D **60**, 014001 (1999)
- [17] T. Hahn, Comput. Phys. Commun. **140**, 418 (2001).
- [18] R. Mertig, M. Böhm, and A. Denner, Comput. Phys. Commun. **4**, 345 (1991).
- [19] T. Hahn and M. Perez-Victoria, Comput. Phys. Commun. **118**, 153 (1999).
- [20] D. s. Du and Z. Wang, Phys. Rev. D **39**, 1342 (1989).
- [21] P. Colangelo, G. Nardulli and N. Paver, Z. Phys. C **57**, 43 (1993).
- [22] V. V. Kiselev and A. V. Tkabladze, Phys. Rev. D **48**, 5208 (1993).

- [23] V. V. Kiselev, A. K. Likhoded and A. I. Onishchenko, Nucl. Phys. B **569**, 473 (2000) Phys. Atom. Nucl. **63** (2000) 2123 [Yad. Fiz. **63** (2000) 2219].
- [24] M. A. Nobes and R. M. Woloshyn, J. Phys. G **26**, 1079 (2000)
- [25] M. A. Ivanov, J. G. Korner and P. Santorelli, Phys. Rev. D **63**, 074010 (2001)
- [26] V. V. Kiselev, A. E. Kovalsky and A. K. Likhoded, Nucl. Phys. B **585**, 353 (2000) V. V. Kiselev, arXiv:hep-ph/0211021
- [27] D. Ebert, R. N. Faustov and V. O. Galkin, Phys. Rev. D **68**, 094020 (2003) D. Ebert, R. N. Faustov and V. O. Galkin, Eur. Phys. J. C **32**, 29 (2003).
- [28] M. A. Ivanov, J. G. Korner and P. Santorelli, Phys. Rev. D **71**, 094006 (2005) [Erratum-ibid. D **75**, 019901 (2007)]
- [29] E. Hernandez, J. Nieves and J. M. Verde-Velasco, Phys. Rev. D **74**, 074008 (2006).
- [30] F. Zuo and T. Huang, Chin. Phys. Lett. **24**, 61 (2007) Eur. Phys. J. C **51**, 833 (2007).
- [31] J. F. Sun, D. S. Du and Y. L. Yang, arXiv:0808.3619.
- [32] R. Dhir, N. Sharma and R. C. Verma, J. Phys. G **35**, 085002 (2008); R. C. Verma and A. Sharma, Phys. Rev. D **65**, 114007 (2002); R. Dhir and R. C. Verma, arXiv:0810.4284
- [33] W. Wang, Y. L. Shen, C. D. Lu, Phys. Rev. **D79**, 054012 (2009).